Phase control of chaotic maps

Sijo K. Joseph and Miguel A. F. Sanjuán

Abstract The phase control method on the dissipative standard map and the Hénon map is studied. We observe that the phase of the control signal can suppress or enhance the chaotic behavior in the bouncing ball map and in Hénon map. We analyze the crisis induced intermittency in the bouncing ball system when the phase of the control signal is varied, also the scaling behavior of the average Lyapunov exponent near the phase induced crisis is studied. Future applications of the phase control method are also discussed.

1 Introduction

The term control of chaos is used mostly to denote the area of studies lying at the interfaces between the control theory and the theory of dynamical systems. The important characteristic of a chaotic dynamical system is the exponential sensitivity to the initial conditions. Even arbitrary close trajectories diverge with time at a finite distance, thus the long term predictions are impossible. This is called butterfly effect as concocted by Philip Merilees

> Does the flap of butterfly's wings in Brazil set off tornado in Texas ?

If that is true, our natural counter question is, what happens when an another butterfly flaps its wings, will the effect get canceled ? Our answer is yes.

Yorke and his collaborators discovered that by a very small variation of a system parameter, it is possible to transform a chaotic trajectory into periodic one and vice versa [20]. In their paper, the parameter is varied by means of a feed back. In the subsequent publication this effect was confirmed experimentally.

Sijo K. Joseph and Miguel A. F. Sanjuán,
Nonlinear Dynamics, Chaos and Complex Systems Group, Departamento de Física
Universidad Rey Juan Carlos, Tulipán s/n, 28933 Móstoles, Madrid, Spain, e-mail: sijo.joseph@urjc.es, miguel.sanjuan@urjc.es

Instead of the conclusion that chaos cannot be fore-casted, but can be controlled gave rise to an explosive interest to researchers. Despite numerous publications on this field, only few strict facts were established, and many issues remain open. In view of the wide scope of possible applications, this area is of interest both to the theorists and Control Engineers [1, 8, 28].

1.1 Phase control method

Chaos control methods are usually classified within two categories, depending on how they interact with the chaotic system. The first category corresponds to feed-back methods, which are aimed to stabilize one of the stable orbits that lie in the chaotic attractor by applying small perturbations that depend on the time-varying state of the system. The experimental implementation of the feedback methods are hard to achieve since it demands fast response to the time variation of the system state. For this reason, non-feedback methods have appeared more useful in many practical cases. The non-feedback methods allow to switch between different dynamical behaviors by applying either parameter perturbations or external forcing signals that do not depend on the current state of the system [3, 14, 22].

We are focusing on a non-feedback control technique called phase control method [28]. This technique has been used to control the chaotic behavior of a Duffing oscillator [26] to control intermittencies [27] and to avoid escapes in a nonlinear oscillator [23]. Similar ideas have been also applied in the context of Josephson junctions [4, 5] and in population dynamics in Theoretical Ecology [11].

Nonfeedback methods have been mainly used to suppress chaos in periodically driven dynamical systems.

$$\dot{\mathbf{x}} = \mathbf{f}(\mathbf{x}, \mathbf{p}) + \mathbf{F}\cos(\omega t), \tag{1}$$

where $\mathbf{x}, \mathbf{f}$ and $\mathbf{F}$ are vectors of the $m-$dimensional phase space, and $\mathbf{p}$ is the parameter vector of the system. The main idea of these nonfeedback methods is to apply a harmonic perturbation either to some of the parameters of the system

$$\dot{\mathbf{x}} = \mathbf{f}(\mathbf{x}, p_i(1 + \varepsilon\cos(r\omega t + \phi)), p_j) + \mathbf{F}\cos(\omega t) \tag{2}$$

for $j = 1\dots n$ being $j \neq i$, or as an external additional forcing to the system,

$$\dot{\mathbf{x}} = \mathbf{f}(\mathbf{x}, \mathbf{p}) + \mathbf{F}\cos(\omega t) + \varepsilon\mathbf{u}\cos(r\omega t + \phi), \tag{3}$$

where $\mathbf{u}$ is conveniently chosen as a unitary vector. Here r determines the ratio between the frequency of the forcing and the natural frequency of the system, and ϕ is the phase difference between the natural oscillation and the forcing signal.

In resonant parametric perturbation methods, the numerical and experimental explorations have been essentially focused on the role played by the perturbation amplitude ε and the resonance condition r, but the role of phase difference ϕ has

hardly been explored. However it is observed that the phase difference ϕ between the periodic forcing and the perturbation have certain influence on the dynamical behavior of the system. The type of control based on varying the phase difference ϕ in search of a desired dynamical behavior is known as the phase control technique.

2 Dissipative maps

In dissipative maps the phase space volume is not conserved. The phase-space volume shrinks as time proceed. Hence the value of the Jacobian is less than one. In area preserving maps the value of the Jacobian is unity. In area preserving maps we cannot observe a definite chaotic attractor. However in a dissipative map we can observe a definite chaotic attractor. We are going to study two different dissipative chaotic maps called, the dissipative bouncing ball map and the Hénon map which are the two simple paradigmatic models for the dissipative map.

2.1 Bouncing ball map

An acceleration mechanism of cosmic ray particles interacting with the time-dependent magnetic field was proposed by Fermi in 1949 [7]. This phenomenon was explained later in terms of a simple classical model by Stanislaw Ulam [25]. Afterward this model became popular as the Fermi-Ulam model [18] and several modified versions were proposed over the years because of its interesting dynamical properties [2, 17]. Among the different models, the simplest one that displays chaotic behavior is the system with one ball bouncing on a vibrating table under the action of gravity. This is widely known as the bouncing ball system [12, 13].

In simple bouncing ball model, a ball is bouncing on a sinusoidally vibrating table under the action of gravity. The evolution of the bouncing ball system is a mix of continuous and discrete evolution. In between the collisions the evolution of the system is continuous but it is discontinuous at the time of collision. Using this property we can easily make a discrete map of the system by analyzing the impact time series. Let $X(t)$ be the position of the ball with respect to the ground reference frame then the series $X(t_0), X(t_1), X(t_2), ..., X(t_n)$, represents the impact time position series of the ball.

Let $\bar{V}_k$ be the velocity of the ball with respect to the fixed reference frame, just after the time of impact t_k and $\bar{V}_k'$ be the velocity just before the impact time t_k. The nature of the impact is relevant, so that if the impact between table and the ball is inelastic we have

$$\bar{V}_k = -\alpha \bar{V}_k', \tag{4}$$

where α is the coefficient of restitution $0 < \alpha \leq 1$, when $\alpha = 1$ the collision is completely elastic. We are interested in the quantities which are in the ground frame

of reference. Considering the $k+1$ collision, consequently we will get

$$\bar{V}_{k+1} = -\alpha\bar{V}'_{k+1}, \tag{5}$$

$$\bar{V}_{k+1} = V_{k+1} - U_{k+1}, \tag{6}$$

$$\bar{V}'_{k+1} = V'_{k+1} - U_{k+1}. \tag{7}$$

Where U_{k+1} is the velocity of the vibrating table at the $k+1$-th collision. Substituting Eq. (6) and Eq. (7) in Eq. (5) we get

$$V_{k+1} - U_{k+1} = -\alpha(V'_{k+1} - U_{k+1}),$$

$$V_{k+1} = (1+\alpha)U_{k+1} - \alpha V'_{k+1}. \tag{8}$$

The variable t represents the instantaneous time between two adjacent collisions $(t_k \leq t \leq t_{k+1})$, where t_k is the time of the k-th impact on the table, and t_{k+1} is the time of the $(k+1)$-th one. Let $X(t)$ be the vertical position of the ball in the ground frame of reference, then according to Newton's law the instantaneous position of the ball is given by,

$$X(t) = X_k + V_k(t - t_k) - \tfrac{g}{2}(t - t_k)^2 \tag{9}$$

and the velocity of the table is given by,

$$V_{k+1} = \frac{dX}{dt}\Big|_{t=t_{k+1}}. \tag{10}$$

Now we can compute the impact velocity equation. The table position is given by $s(t) = A\sin(\omega t + \theta_0)$. Thus our table velocity is given by

$$U_{k+1} = \frac{ds}{dt}\Big|_{t=t_{k+1}}. \tag{11}$$

The instantaneous distance between the table and the ball is given by $d(t) = x(t) - s(t)$. We can find the impact time by solving $d(t_{k+1}) = 0$ since impact occurs when the distance between the table and the ball goes to zero. Therefore

$$X_k + V_k(t_{k+1} - t_k) - \frac{1}{2}g(t_{k+1} - t_k)^2$$
$$-A\sin(\omega t_{k+1} + \theta_0) = 0. \tag{12}$$

The above equation is called the time recurrence equation. If we substitute $U_k = A\omega\cos(\omega t_k + \theta_0)$ and $V'_{k+1} = V_k - g(t_{k+1} - t_k)$ in Eq. (8), we can obtain Eq. (13), which is the recurrence velocity equation

$$V_{k+1} = (1+\alpha)A\omega\cos(\omega t_{k+1} + \theta_0)$$
$$-\alpha[V_k - g(t_{k+1} - t_k)]. \tag{13}$$

The complete recurrence equations are given by

$$X_k + V_k(t_{k+1} - t_k) - \frac{1}{2}g(t_{k+1} - t_k)^2$$
$$-A\sin(\omega t_{k+1} + \theta_0) = 0, \tag{14}$$

$$V_{k+1} = (1 + \alpha)A\omega\cos(\omega t_{k+1} + \theta_0)$$
$$-\alpha[V_k - g(t_{k+1} - t_k)]. \tag{15}$$

These are the exact time and velocity recurrence equations, respectively. But one of them is explicit and another one is implicit. Since we want to construct a non-linear map out of these equations, we need both equations to be explicit. To solve this problem we make use of an approximation, which is called the high bounce approximation.

2.1.1 High bounce approximation

In this approximation we assume that the bouncing height of the ball is large compared with the vibration of the table. Thus we say that the velocity of the ball simply change its sign for the $k+1$-th collision. Therefore,

$$V'_{k+1} = -V_k. \tag{16}$$

But using the equation of motion we have,

$$V'_{k+1} = V_k - g(t_{k+1} - t_k). \tag{17}$$

Substituting Eq. (16) in Eq. (17) we have,

$$t_{k+1} = t_k + \frac{2V_k}{g}. \tag{18}$$

Thus the approximated explicit recurrence equations are given by

$$t_{k+1} = t_k + \frac{2V_k}{g}, \tag{19}$$
$$V_{k+1} = (1 + \alpha)A\omega\cos(\omega t + \theta_0) - \alpha[V_k - g(t_{k+1} - t_k)].$$

If we transform Eq. (19) and Eq. (20) to make them dimensionless by changing variables as $x_k = \omega t_k + \theta_0, \quad y_k = (2\omega/g)V_k, \quad \beta = (2\omega^2 A/g)(1 + \alpha)$ we get,

$$\begin{aligned} x_{k+1} &= x_k + y_k \\ y_{k+1} &= \beta\cos x_{k+1} - \alpha[y_k - 2(x_{k+1} - x_k)]. \end{aligned} \tag{20}$$

If we substitute the phase equation $x_{k+1} = x_k + y_k$ in Eq. (20) we get the complete approximated explicit recurrence equations, which is given by,

$$\begin{aligned}
x_{n+1} &= x_n + y_n \\
y_{n+1} &= \alpha y_n + \beta \cos(x_n + y_n)
\end{aligned} \tag{21}$$

Here x is associated with the time interval between collisions and y is associated with the velocity of the ball just after the impact. Here α is the coefficient of restitution. Jacobian matrix of a two dimensional map is defined by

$$J = \frac{\partial(x_{i+1}, y_{i+1})}{\partial(x_i, y_i)} \tag{22}$$

Thus the Jacobian matrix of the bouncing ball map is given by,

$$J = \begin{bmatrix} 1 & 1 \\ \beta S & \alpha + \beta S \end{bmatrix}$$

where $S = \sin(x_k + y_k)$. In order to calculate the dissipation effect, let us take determinant of the Jacobian matrix, which is given by,

$$|J| = \begin{vmatrix} 1 & 1 \\ \beta \sin(x_k + y_k) & \alpha + \beta \sin(x_k + y_k) \end{vmatrix}$$

$$|J| = \alpha \tag{23}$$

Here in dissipative bouncing ball model we are considering the inelastic collisions of the ball with the table. Hence the energy is not conserved. The energy loss is determined by the dissipation coefficient α. Hence, it is evident that α is the dissipation coefficient so here α gives the measure of the contraction of phase space.

Eigenvalues of the Jacobian matrix is given by,

$$\Lambda^2 - \Lambda\, Tr(J) + |J| = 0, \tag{24}$$

$$\tag{25}$$

where $Tr(J)$ means the trace of the matrix J. Thus, by solving this equation,

$$\Lambda = \frac{1}{2}[\quad (1 + \alpha + \beta S) \pm \sqrt{(1 + \alpha + \beta S)^2 - 4\alpha}], \tag{26}$$

where $S = \sin(X_k + Y_k)$, and Λ are the local Lyapunov exponents. The global Lyapunov exponents are defined as,

$$\lambda_j = \lim_{n \to \infty} \frac{1}{n} \ln|\Lambda_j|, \quad j = 1, 2, \tag{27}$$

where Λ_j are the eigenvalues of $M = \prod_{i=1}^{n} J_i(X_i, Yi)$. If the value of λ_j is positive, then the phase space trajectories diverge exponentially, which in turn gives the chaotic behavior in the system.

Since bouncing ball system is a dissipative one there exist a definite chaotic attractor, which is shown in Fig. 1. Here the width of the attractor depends on the dissipation coefficient α. If the value of α is closer to zero the width of the attractor is minimum and the width is maximum when the value of the alpha is closer to unity. If the value of the dissipation coefficient α reaches unity then the specific chaotic attractor vanishes and the system shows Hamiltonian chaos.
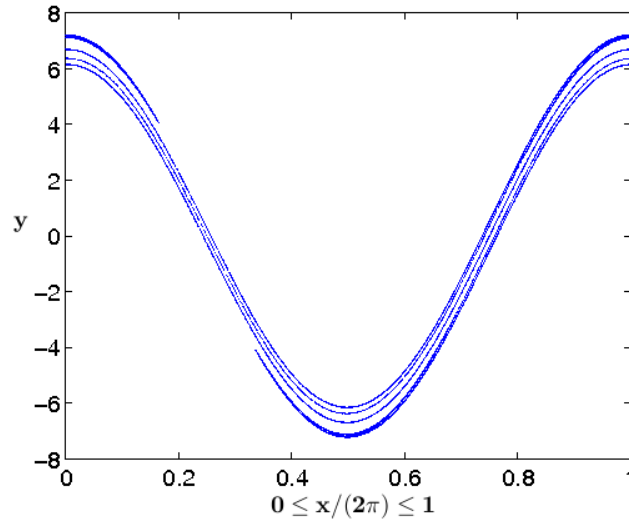

Fig. 1 The figure shows the chaotic attractor of the dissipative boucing ball map. Here we have taken the parameter values $\alpha = 0.1$ and $\beta = 6.56$.

2.1.2 Standard map

If the coefficient of restitution is unity then the dissipative bouncing ball map reduces to standard map.

$$
\begin{aligned}
x_{n+1} &= x_n + y_n \\
y_{n+1} &= y_n + \beta \cos(x_n + y_n)
\end{aligned}
\tag{28}
$$

This is an area preserving map since the determinant of the Jacobian matrix is unity. This is one of the important chaotic map studied in connection with the kicked rotor.

2.2 Hénon map

Lorentz system consists of three first-order differential equations, whose solutions tend toward a strange attractor called Lorentz attractor. Hénon's orginal idea was to replace these first-order differential equations by a simple two dimensional map which shows the same properties of the Lorentz system. He was inspired by the work of the numerical results of Pomeau on the Lorentz system, which shows clearly how a volume is stretched in one direction, and at the same time folded over itself, in the course of one revolution.

We are going to consider Hénon's original derivation of the map [15]. Consider a region elongated along x axis, we begin the folding by,

$$T' : x' = x, \ y' = y + 1 - ax^2. \tag{29}$$

We complete the folding by a contraction along the x axis,

$$T'' : x'' = bx', \ y'' = y'. \tag{30}$$

Finally we come back to the orientation along x axis by,

$$T''' : x''' = y'', \ y''' = x''. \tag{31}$$

The final mapping will be defined as the product $T = T'''T''T'$. If we write (x_n, y_n) for (x, y) and (x_{n+1}, y_{n+1}) for (x''', y''') Then we have,

$$\begin{aligned} x_{n+1} &= y_n + 1 - ax_n^2 \\ y_{n+1} &= bx_n \end{aligned} \tag{32}$$

The above map is called Hénon map, but we use slightly different version of the Hénon map, which is given by,

$$\begin{aligned} x_{n+1} &= A + By_n - x_n^2 \\ y_{n+1} &= x_n \end{aligned} \tag{33}$$

This is one of the important examples of dynamical systems that exhibit chaotic behavior. Here A and B are the parameters of the map. The Jacobian of the map is given by,

$$|J| = \begin{vmatrix} -2x_n & B \\ 1 & 0 \end{vmatrix}$$

Hence the jacobian is given,

$$|J| = -B \tag{34}$$

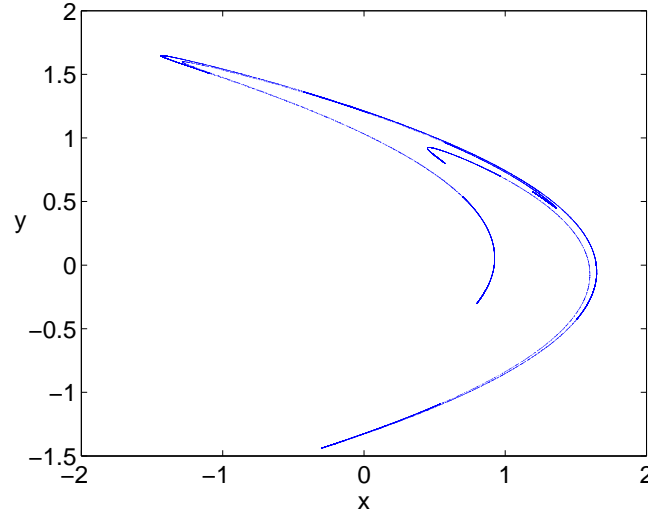Here $-B$ is the measure of contraction of the phase-space area in the Hénon map.

Fig. 2 The figure shows the chaotic attractor for the Hénon map. Here we take the parameter values $A = 1.3$ and $B = 0.285$

We can observe a definite chaotic attractor in a Hénon map. The chaotic attractor for the Hénon map is shown in Fig. 2.

3 Phase control of chaos

Now we are going to apply the phase control method on nonlinear chaotic maps called the dissipative bouncing ball map and the Hénon map. The key idea of the phase control method is to apply a harmonic external perturbation to one of the variables of the map. It is possible to control chaos in the system simply by tuning the phase of the external perturbation.

3.1 Control of chaos in the bouncing ball map

We apply the phase control method on bouncing ball map Eq. (21), by adding an external harmonic perturbation to the parameter β. Finally the equation used for the numerical exploration of our technique reads,

$$
\begin{aligned}
x_{n+1} &= x_n + y_n \\
y_{n+1} &= \alpha y_n + \beta \left(1 + \varepsilon \sin(2\pi r n + \phi) \right). \\
&\quad \times \cos(x_n + y_n),
\end{aligned}
\tag{35}
$$

where ε, ϕ and r are used as free parameters, and $\alpha = 0.1$ is fixed throughout the calculation. When the forcing amplitude ε is zero, this map reduces to the simple bouncing ball map.

One of the key ideas of this control technique consists in assuming that the external perturbation is of small amplitude, so that once we may fix r and for a considerably small value of parameter ε, we may use only ϕ as a free parameter to control the system. Physically it means we are adding an external small sinusoidal perturbation on the table frequency and changing only the phase of the applied control signal.

In order to analyze the effect of phase control on bouncing ball system, first we have to observe the dynamics of the system without the control. In bouncing ball system chaos appears as a result of period doubling

Thus we have analyzed the bifurcation diagram of the unperturbed bouncing ball system by changing the value of parameter β. This is shown in the Fig. 3, where we can see some regions of chaotic behavior and some periodic windows. For example, the one centered at $\beta = 6$ and the one centered at $\beta = 10.3$. If we apply our phase
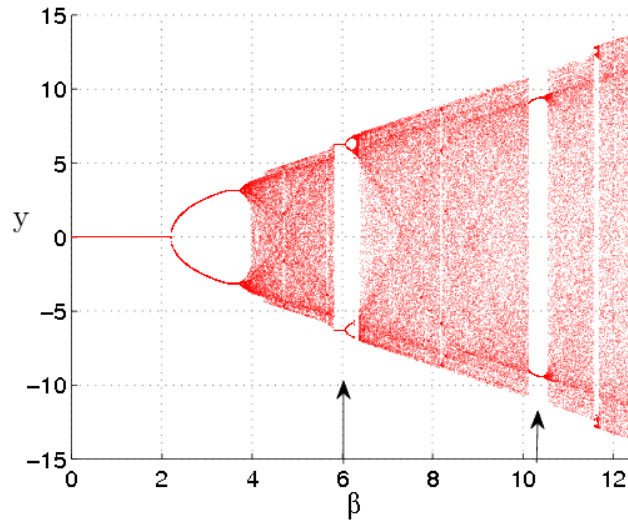

Fig. 3 The figure shows the bifurcation diagram of the bouncing ball system, by varying the parameter β. Here we can observe two wide periodic windows at $\beta = 6$ and at $\beta = 10.3$.

control method it is possible to change the behavior of the system from chaotic to periodic and vice versa. Thus we simply start with parameter values which give chaotic dynamics in the unperturbed bouncing ball system. In order to evaluate in a detailed way the role of ε and ϕ, we calculate the largest Lyapunov exponent over every point in a 200×200 grid in the rectangle of the parameter plane $0.02 \leq \varepsilon \leq 0.07$, $0 \leq \phi \leq 2\pi$, fixing r for each computation, which is shown in Fig. 4. We
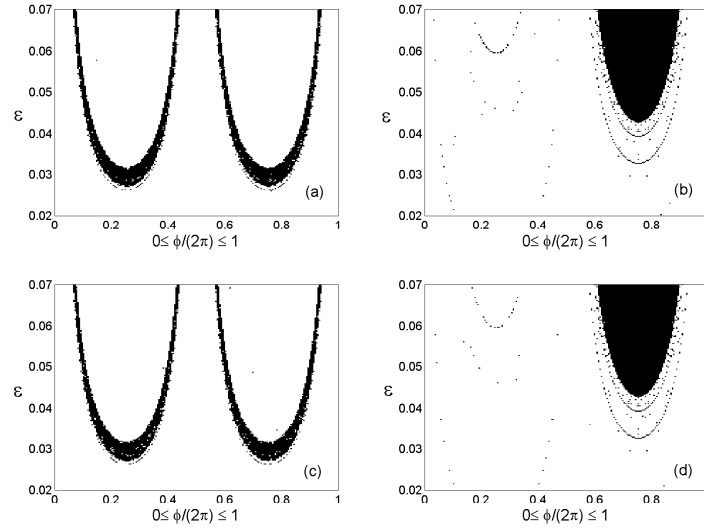
Fig. 4 The figure shows the sign of the largest Lyapunov exponent λ computed at every point of a 200×200 grid of (ε, ϕ) values. The range of variation is $0 \leq \phi \leq 2\pi, 0.02 \leq \varepsilon \leq 0.07$ for different values of the resonant condition, $(a) : r = 0.5, (b) : r = 1.0, (c) : r = 1.5, (d) : r = 2.0$. The Lyapunov exponent is negative in the black regions. These regions have a structure that follows the expected symmetry around $\phi = \pi$ when r is an odd multiple of 0.5 and the trivial symmetry around $\phi = 2\pi$ for an even multiple of 0.5. We set the parameters $\beta = 6.56, \alpha = 0.1$.

consider that the perturbation acting on the system is small, and consequently this requires small values of ε. As we are searching for areas in the parameter plane where the transition between chaotic and regular motion takes place, we take care of transient states by waiting for a sufficiently long time to fix the corresponding stable regime. We plot the results of several integer and half integer r values. The black and white color associated to each point in the (ε, ϕ) plane indicate the sign of the largest Lyapunov exponent. If it is greater than zero (white region) then the dynamics is chaotic, and if it is less than zero (black region) then the system shows a regular periodic behavior.

Figure 4 shows that there exist wide regions of the (ε, ϕ) plane where λ is smaller than zero, and therefore chaos is suppressed. We note that the control regions, far from having a trivial or irregular shape, present a symmetry that depends on the parity of the r parameter. The π symmetry when r is odd an multiple of 0.5 and 2π symmetry when r is even multiples of 0.5. The most interesting feature is the role of the phase ϕ in selecting the final state of the system. From Fig. 4(a) we can see that we have a periodic behavior for the parameter value at $\phi = \pi/2, \varepsilon = 0.03$. Thus, we fix these values and search for the system behavior, thus we have plotted the bifurcation diagram Fig. 5 by fixing $\phi = \pi/2, \varepsilon = 0.03, \alpha = 0.1$. Numerically it is observed that by a proper choice of the frequency of the controlling signal and a

suitable phase difference ϕ it is possible to avoid chaos in the bouncing ball system.
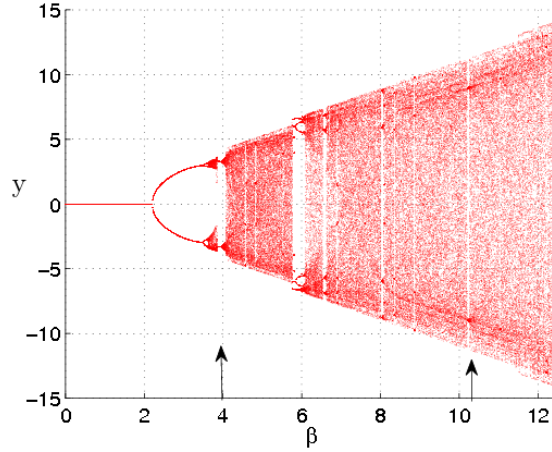

Fig. 5 The figure shows the bifurcation diagram of the bouncing ball system when the phase control is applied. On the y-axis we have the velocity of the bouncing ball. We see that a new periodic window arises under perturbation when $\beta = 4$, at the same time the periodic window centered at $\beta = 10.3$ disappears. Here the perturbation parameters are taken as $\alpha = 0.1$, $r = 0.5$, $\varepsilon = 0.03$ and $\phi = \pi/2$.

We can observe other interesting phenomena like the appearance as well as the disappearance of periodic windows in the bifurcation diagram. Let us compare the bifurcation diagram without the pertubation (Fig. 3) with the bifurcation diagram when the perturbation is applied (Fig. 5). Thus we can observe that, in Fig. 5 a new periodic window arises around $\beta = 4$ and at the same time we can observe that the periodic window centered at $\beta = 10.3$ is vanished. Thus this interesting phenomenon is particularly useful to generate chaos as well as to suppress chaos in a dynamical system. If we operate our system near the parameter range where new periodic windows arise when periodic perturbation is applied, we can easily control chaos. If the system is operating in a periodic window which vanishes on periodic perturbation, then we can generate chaos in the system under the periodic perturbation. Thus this interesting phenomenon helps us to switch the system behavior from chaotic to periodic and vice versa.

3.2 Control of chaos in Hénon map

In order to apply our phase control technique in the Hénon map Eq. (21), we add a harmonic perturbation $\varepsilon \sin(2\pi r n + \phi)$ to the parameter B. Finally the equation used
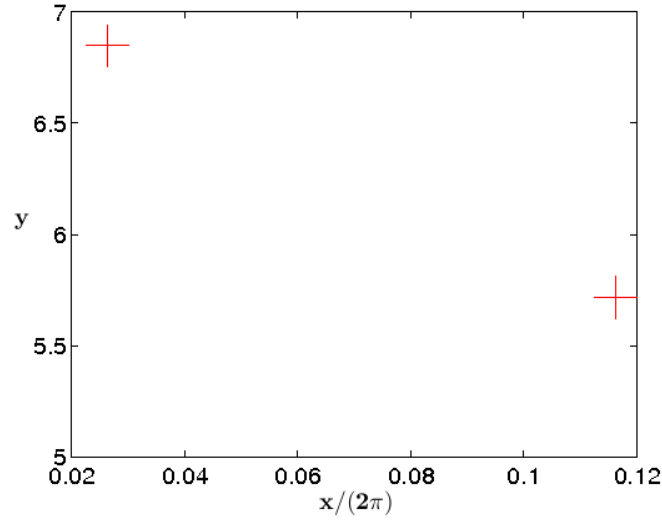
Fig. 6 The figure shows the period two attractor in the phase space of the bouncing ball system when the periodic perturbation is applied. When the periodic perturbation is absent, the bouncing ball map shows a chaotic attractor which is shown in Fig. 1. Here we take the parameter values $\alpha = 0.1, \beta = 6.56, \varepsilon = 0.03, r = 0.5, \phi = 1.57$.

for the numerical exploration of the technique reads,

$$
\begin{aligned}
x_{n+1} &= A + B(1 + \varepsilon \sin(2\pi r n + \phi))y_n - x_n^2 \\
y_{n+1} &= x_n
\end{aligned}
\tag{36}
$$

In order to suppress chaos, we have to search for the suitable ε, ϕ values in the Eq. (36). In order to analyze the effect of phase control on Hénon map, we simply start with parameter values which give chaotic dynamics in the unperturbed Hénon map.

In order to evaluate in a detailed way the role of ε and ϕ, we calculate the largest Lyapunov exponent over every point in a 200×200 grid in the rectangle of the parameter plane $0.003 \leq \varepsilon \leq 0.006$, $0 \leq \phi \leq 2\pi$, fixing r for each computation, which is shown in Fig. 7. Note that as we explained before, we consider that the perturbation acting on the system is small, and consequently this requires small values of ε.

As we are searching for areas in the parameter plane where the transition between chaotic and regular motion takes place, we take care of transient states by waiting for a sufficiently long time to fix the corresponding stable regime. We plot the results of several integer and half integer r values. The black and white color associated to each point in the (ε, ϕ) plane indicate the sign of the largest Lyapunov exponent. If it is greater than zero (white region) then the dynamics is chaotic, and if it is less than zero (black region) then the system shows a regular periodic behavior.
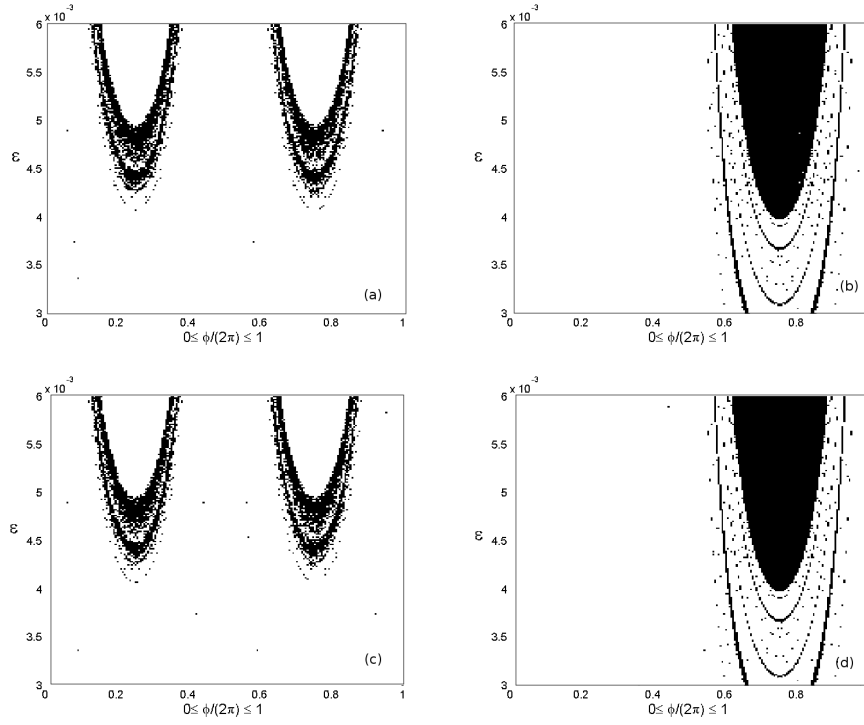
Fig. 7 The figure shows the sign of the largest Lyapunov exponent λ computed at every point of a 200×200 grid of (ε, ϕ) values. The range of variation is $0 \leq \phi \leq 2\pi, 0.003 \leq \varepsilon \leq 0.006$ for different values of the resonant condition, $(a) : r = 0.5, (b) : r = 1.0, (c) : r = 1.5, (d) : r = 2.0$. The Lyapunov exponent is negative in the black regions. These regions have a structure that follows the expected symmetry around $\phi = \pi$ when r is an odd multiple of 0.5 and the trivial symmetry around $\phi = 2\pi$ for an even multiple of 0.5. Here we take $A = 1.3, B = 0.285$

Figure 7 shows that there exist wide regions of the (ε, ϕ) plane where λ is smaller than zero, and therefore chaos is suppressed. The control regions, far from having a trivial or irregular shape, present a symmetry that depends on the parity of the r parameter. The π symmetry when r is odd multiples of 0.5 and 2π symmetry when r is an even multiple of 0.5. The most interesting feature is the role of the phase ϕ in selecting the final state of the system. From Fig. 7(a) we can see that we have a periodic behavior for the parameter value at $\phi = \pi/2, \varepsilon = 0.00475$. Thus, we fix these values and search for the system behavior, thus we have plotted the phase-space diagram in Fig. 8 by fixing $A = 1.3, B = 0.285, \phi = \pi/2, \varepsilon = 0.00475$. Here we can see that the chaotic Hénon attractor (shown in Fig. 2) turned into an orbit of period-14 (shown in Fig. 8). Numerically it is observed that by a proper choice of the phase difference ϕ it is possible to avoid chaos in Hénon map.
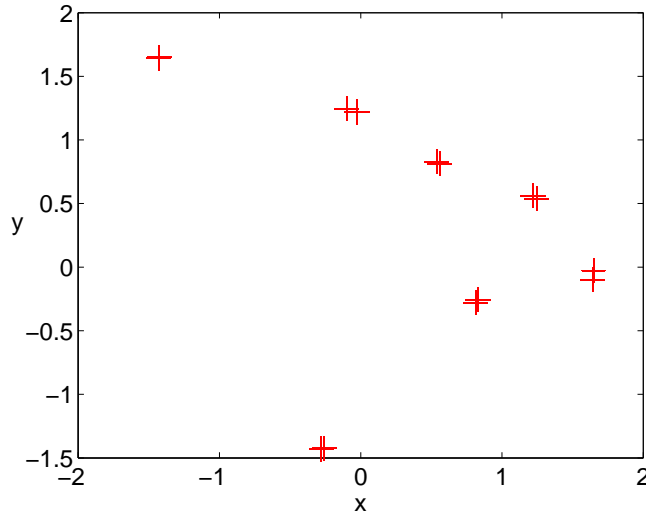
Fig. 8 The figure shows the period 14 attractor when the external periodic perturbation is applied. When the external perturbation is absent, the system shows a chaotic attractor which is shown in Fig. 2. Here we have taken the parameter values $A = 1.3$, $B = 0.285$, $\varepsilon = 0.00475$, $\phi = \pi/2$ and $r = 0.5$

4 Phase dependent intermittency and crisis

When the control parameter is modified a chaotic attractor can touch an unstable periodic orbit inside its basin of attraction, then a sudden expansion of the chaotic attractor is observed. This phenomenon is called interior crisis. Beyond the crisis the system preserves a memory of the former situation, thus a fraction of the time is spent in the region corresponding to the pre-crisis attractor, and during the rest of the time excursions around the formerly unstable periodic orbit take place. This behavior is known as crisis induced intermittency. Before the crisis, such excursions cannot take place unless noise or external perturbation induces them. We show that the intermittency at an interior crisis can be controlled by our phase control method. We give a numerical evidence that if we choose a proper parameter value it can be used to enhance the crisis. Experimental and theoretical study of phase control of intermittency was already tested successfully in a laser system by Zambrano *et al* [27].

4.1 Intermittency in bouncing ball map

In order to analyze the effect of phase ϕ and forcing amplitude ε on crisis, we are scanning over the possible ϕ and ε values to determine the region where the crisis

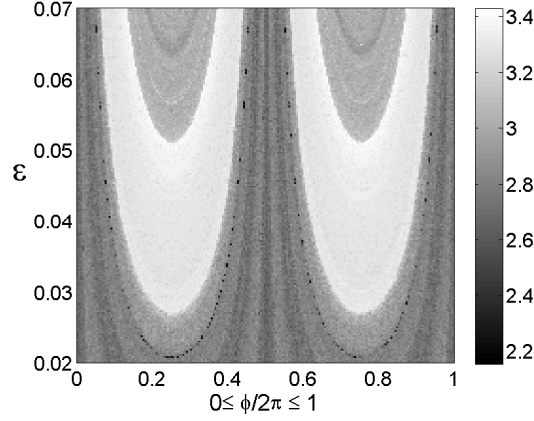**Fig. 9** The figure shows the average value of the relative maxima of the velocity, $<H>$, computed at every point of a 200×200 grid of (ε, ϕ) values in the region $0 \leq \phi \leq 2\pi, 0.02 \leq \varepsilon \leq 0.07$ for the perturbed bouncing ball map. The white region shows the sudden expansion in the attractor. Here we set the parameters $\alpha = 0.1$, $\beta = 4.05$ and $r = 0.5$.

is induced. A good indicator to discriminate between the different dynamical states of the system for different values of the parameter is

$$<H>=<\max(y_n)>|_{y_n>y_0},\qquad(37)$$

where $<H>$ gives the average value of the maximum of the time series of y_n. In other words $<H>$ is the average value of the relative maximum velocity of the bouncing ball just after the impact. The value of y_0 is chosen in such a way that $<H>$ enables us to distinguish between the chaos and the intermittent regime. In the numerical simulations, we have observed that taking $y_0 = 10^{-6}$, that is, neglecting only extremely small peaks of the signal, is sufficient for this discrimination.

In Fig. 9 the wide symmetrical white regions shows that there is an expansion in the attractor. But that exist only for some specific values of the parameters. We can see that there is a range of phase values (white regions) give a sudden expansion in the attractor, which in turn leads to intermittency. There exist a symmetry in the phase value of the applied signal which induces the internal crisis in the system. This can be explained in terms of symmetry of the map under the transformation $\phi \rightarrow \phi + \pi/2$. This symmetry depends on the frequency ratio r. In order to gain a deeper insight into the role of ϕ in nonlinear systems we study the effect of phase on the perturbed map close to an interior crisis. From Fig. 10(a) and Fig. 10(b) we can observe the sudden expansion of the attractor. From Fig. 10(b) the enlarged attractor consists of the attractor in the pre-crisis regime and the enlarged dotted region gives the intermittency. Since the dotted region gives the leaking trajectories from one piece of the attractor to another. Here the phase change enhance crisis in the system which inturn induce intermittency in the system. One of the interesting aspect to study is the scaling property of the phase close to the critical point after the occur-
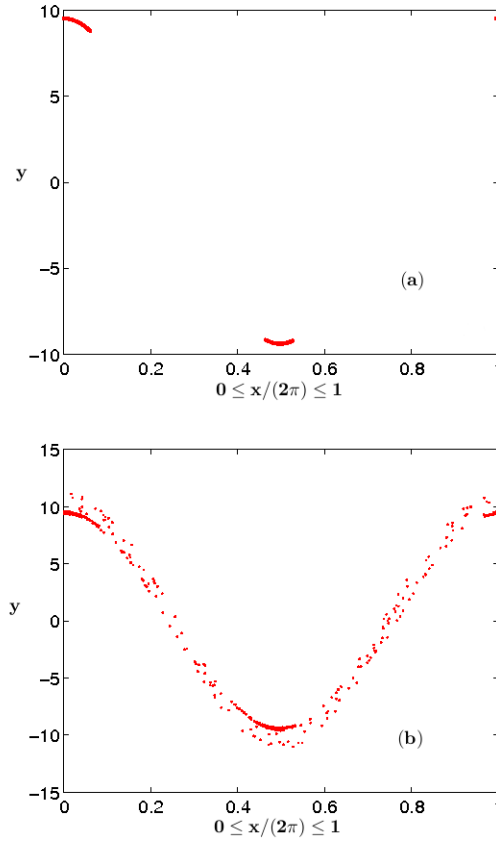
Fig. 10 (a) Shows the chaotic three piece attractor just before ($\phi = 0.27650$) the interior crisis. (b) Shows the enlarged attractor just after interior crisis ($\phi = 0.27660$). Thus the system has an interior crisis at $\phi_c \approx 0.27655$. The dense points in the enlarged attractor gives the attractor in the pre-crisis regime and the enlarged dotted region gives the intermittency. Here we fix $\alpha = 0.1$, $\beta = 10.4$, $\varepsilon = 0.03$

rence of crisis. In this post-crisis regime the dynamics describing the evolution of the system is intermittent. A scaling law for the mean time a chaotic orbit spends in the region of the precrisis attractor ($< \tau >$), as the control parameter (ϕ) is varied had been proposed by Grebogi et al [10]. It is found that $< \tau >$ decreases according to the scaling relation $< \tau > \sim |\phi - \phi_c|^{-\gamma}$ where γ is the scaling exponent describing the scaling of $< \tau >$ with a parameter ϕ. The behavior of lyapunov exponents near crisis point for the dissipative standard map had been studied B. Pompe and R. W. Leven [21]. According to them the increase of the largest lyapunov exponent near crisis is a consequence of the rapid growth of the transition probability . Thus we can say that the mean time of a chaotic orbit spends in the region $< \tau >$ is inversely proportional to the lyapunov exponents. In other words the size of the
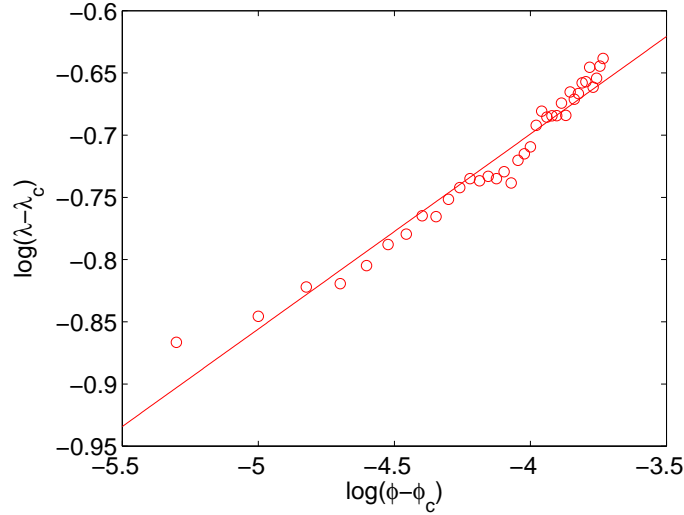
Fig. 11 The figure shows the graph of the $\log(\lambda - \lambda_c)$ versus $\log(\phi - \phi_c)$. The slope of the linear best fit yields the value of the scaling exponent $\gamma = 0.15$ with a norm of residuals 0.07. Here the phase of the control signal gives the same scaling behaviour like a normal parameter. Here we vary ϕ from 0.276615 to 0.276800 with an increment of 5×10^{-6}.

attractor is related to the lyapunov exponent via Kaplan-Yorke dimension. Thus the new scaling equation reads,

$$\lambda(\phi) - \lambda(\phi_c) \sim |\phi - \phi_c|^\gamma \tag{38}$$

This type of scaling law of lyapunov exponent makes an analogy with the phase transition in statistical physics. Till now there isn't any known connection between the statistical quantities and the lyapunov exponent. In the last section numerically we make a connection between the statistical quantity called saturation velocity and the lyapunov exponent. In our case as we know, the phase can enhance the crisis. Thus we analyze the validity of the scaling law of averaged lyapunov exponent versus the phase of the applied signal near the crisis regime. Behaviour of the lyapunov exponent near crisis regime has studied bye several authors [19, 24] Here we calculate the average lyapunov exponent using 10^2 initial conditions calculated over an orbit length of 10^4 iterations. The slope of the linear best fit gives the value of scaling exponent $\gamma = 0.15$ with the norm of residuals 0.07.

5 Phase control method and its future

Complex system can be understood in a better way using Nonlinear Dynamics. Interestingly most of the complex systems exhibit the chaotic behavior. Many mechanical vibrations, irregular oscillations in chemical reactions, and the spread of epidemics are chaotic in nature. In most of these situations chaos is considered as an undesirable property. Hence the idea of controlling chaos is important on these fields.

One of the medical applications of the chaos control is to control the Cardiac Dysrhythmia (Arrhythmia). Arrhythmia is the irregular or chaotic Heart beat due to the abnormal electrical conductivity in the Heart. Celebrated chaos control method called O.G.Y had already been implemented successfully in experimental model of Arrhythmia [9]. Controlling chaotic or irregular mechanical oscillation or vibration is a challenging task for Mechanical Engineers. Chaos control methods had already been applied to stabilize the mechanical vibrations of Helicopter wings [16]. Researchers at Oak Ridge National Labs and the University of Tennessee had applied a two dimensional map based approach to model the cycle variations in spark-ignited combustion engines [6] . The combustion efficiency of an internal combustion engine can vary significantly from one cycle to the next. This cycle variability is enhanced under lean (oxygen rich) fueling. The importance of understanding and controlling cycle variability has increased in recent years, as car manufacturers are trying to run their engines with leaner fuel mixtures to improve fuel efficiency and reduce NO_x emissions. Hence the chaos control methods are promising tools for the future combustion engines.

In all the aforementioned fields the phase control method is rarely explored. One of the greatest advantages of the phase control technique is that, we don't need the prior knowledge of the dynamics of the system. Also the simplicity of its implementation makes this method more attractive. Hence this simple and attractive chaos control technique might be the future of the coming technologies.

References

1. Andrievskii, B.R., Fradkov, A.L.: Control of chaos: Methods and applications. II. applications. Autom. Remote Control **65**, 505–533 (2004)
2. Brahic, H.: Numerical study of a simple dynamical system. 1. the associated plane area-preserving mapping. Astron. Astrophys. **12**, 98–110 (1971)
3. Braiman, Y., Goldhirsch, I.: Taming chaotic dynamics with weak periodic perturbations. Phys. Rev. Lett. **66**(20), 2545–2548 (1991)
4. Chitra, R.N., Kuriakose, V.C.: Dynamics of coupled josephson junctions under the influence of applied fields. Phys. Lett. A **365**(4), 284 – 289 (2007)
5. Chitra, R.N., Kuriakose, V.C.: Phase effects on synchronization by dynamical relaying in delay-coupled systems. Chaos: An Interdisciplinary Journal of Nonlinear Science **18**(2), 023,129 (2008)

6. Daw, C.S., Finney, C.E.A., Green, J.B., Kennely, M.B., Thomasy, J.F.: A simple model for cyclic variations in a spark-ignition engine. No. 962086 in SAE technical paper series. Society of Automotive Engineers (1996)
7. Fermi, E.: On the origin of the cosmic radiation. Phys. Rev. **75**(8), 1169–1174 (1949)
8. Fradkov, A.L., Evans, R.J.: Control of chaos: Methods and applications in engineering. Annual Reviews in Control **29**(1), 33–56 (2005)
9. Garfinkel, A., Spano, M., Ditto, W.L., Weiss, J.: Controlling cardiac chaos. SCIENCE **257**(5074), 1230–1235 (1992)
10. Grebogi, C., Ott, E., Romeiras, F., Yorke, J.A.: Critical exponents for crisis-induced intermittency. Phys. Rev. A **36**(11), 5365–5380 (1987)
11. Greenman, J.V., Pasour, V.B.: Phase control of resonant systems: Interference, chaos and high periodicity. J. Theor. Biol. **278**(1), 74–86 (2011)
12. Guckenheimer, J., Holmes, P.: Nonlinear Oscillations, Dynamical Systems, and Bifurcations of Vector Fields. No. 42 in Applied Mathematical Sciences. Springer-Verlag, New York, NY (1983)
13. Holmes, P.J.: The dynamics of repeated impacts with a sinusoidally vibrating table. Journal of Sound and Vibration **84**(2), 173 – 189 (1982)
14. Hsu, R.R., Su, H.T., Chern, J.L., Chen, C.C.: Conditions to control chaotic dynamics by weak periodic perturbation. Phys. Rev. Lett. **78**(15), 2936–2939 (1997)
15. Hnon, M.: A two-dimensional mapping with a strange attractor. Communications in Mathematical Physics **50**, 69–77 (1976). 10.1007/BF01608556
16. KRODKIEWSKI, J.M., FARAGHER, J.S.: Stabilization of motion of helicopter rotor blades using delayed feedbackmodelling, computer simulation and experimental verification. Journal of Sound and Vibration **234**(4), 591 – 610 (2000)
17. Leonel, E.D., McClintock, P.V.E.: Effect of a frictional force on the fermi-ulam model. J. Phys. A: Math. Gen. **39**, 11,399 (2006)
18. Lieberman, M.A., Lichtenberg, A.J.: Stochastic and adiabatic behavior of particles accelerated by periodic forces. Phys. Rev. A **5**(4), 1852–1866 (1972)
19. Mehra, V., Ramaswamy, R.: Maximal lyapunov exponent at crises. Phys. Rev. E **53**(4), 3420–3424 (1996)
20. Ott, E., Grebogi, C., Yorke, J.A.: Controlling chaos. Phys. Rev. Lett. **64**(11), 1196–1199 (1990)
21. Pompe, B., Leven, R.W.: Behaviour of lyapunov exponents near crisis points in the dissipative standard map. Physica Scripta **38**(5), 651 (1988)
22. Sanjuán, M.A.F.: Using nonharmonic forcing to switch the periodicity in nonlinear systems. Phys. Rev. E **58**(4), 4377–4382 (1998)
23. Seoane, J.M., Zambrano, S., Euzzor, S., Meucci, R., Arecchi, F.T., Sanjuán, M.A.F.: Avoiding escapes in open dynamical systems using phase control. Phys. Rev. E **78**(1), 016,205 (2008)
24. Stynes, D., Hanan, W.G., Pouryahya, S., Heffernan, D.M.: Scaling relations and critical exponents for two dimensional two parameter maps. Eur. Phys. J. B **77**(4), 469–478 (2010)
25. Ulam, S.M.: On some statistical properties of dynamical systems. In: L.M.L. Cam, J. Neyman, E. Scott (eds.) Proceedings of the Fourth Berkeley Symposium on Mathematical Statistics and Probability (University of California, Berkeley, June 20–July 30, 1960), vol. 3, pp. 315–320. University of California Press, Berkeley (1961)
26. Zambrano, S., Brugioni, S., Allaria, E., Leyva, I., Meucci, R., Sanjuán, M.A.F., Arecchi, F.T.: Numerical and experimental exploration of phase control of chaos. Chaos **16**, 013,111 (2006)
27. Zambrano, S., Mariño, I.P., Salvadori, F., Meucci, R., Sanjuán, M.A.F., Arecchi, F.T.: Phase control of intermittency in dynamical systems. Phys. Rev. E **74**(1), 016,202 (2006)
28. Zambrano, S., Seoane, J.M., Mariño, I.P., Sanjuán, M.A.F., Meucci, R.: Phase control in nonlinear systems, chap. 6, pp. 147–188. World Scientific, Singapore (2010)